Magnetic anisotropy in Ce/Fe and Ce/FeCoV multilayers

2001 J. Phys.: Condens. Matter 13 9699

(http://iopscience.iop.org/0953-8984/13/43/303)

INSTITUTE OF PHYSICS PUBLISHING JOURNAL OF PHYSICS: CONDENSED MATTER

J. Phys.: Condens. Matter **13** (2001) 9699–9712 PII: S0953-8984(01)27283-X

Magnetic anisotropy in Ce/Fe and Ce/FeCoV multilayers

G S Case[1], M F Thomas[1], C A Lucas[1], D Mannix[1], P Boni[2], S Tixier[2] and S Langridge[3]

[1] Department of Physics, University of Liverpool, Liverpool L69 7ZE, UK
[2] Laboratory for Neutron Scattering, ETH and PSI, CH-5232 Villigen, Switzerland
[3] ISIS Facility, Rutherford Appleton Laboratory, Chilton, Didcot OX11 0QX, UK

Received 27 July 2001
Published 12 October 2001
Online at stacks.iop.org/JPhysCM/13/9699

Abstract

Multilayer samples of Ce/Fe and Ce/FeCoV, fabricated by sputtering and characterized by means of x-ray diffraction and reflectivity, were studied by ^{57}Fe Mössbauer spectroscopy and polarized neutron reflectivity. In the Ce/Fe system a paramagnetic Fe phase is observed at room temperature for Fe thicknesses below 20 Å. This phase is ordered at 4.2 K, and is attributed to amorphous Fe at the interface with Ce. In contrast, the Ce/FeCoV system is ferromagnetic at room temperature for all layer thicknesses studied. From the relative intensity of the Mössbauer lines we show that both systems exhibit a perpendicular magnetic anisotropy for magnetic layers of less than 17 Å thickness, indicating a positive interface anisotropy constant, K_S. For a selection of Ce/Fe samples, the reorientation of the magnetic moments in magnetic fields applied normal to the layers enabled the magnetic anisotropy energy K_{eff} of each sample to be evaluated. The trend of the values of K_{eff} gave volume and interface anisotropy constants $K_V = 1.1\ (\pm 1.2) \times 10^5\ \mathrm{J\,m^{-3}}$ and $K_S = 0.98\ (\pm 0.15) \times 10^{-3}\ \mathrm{J\,m^{-2}}$ for the Ce/Fe system, where the positive values indicate a preference for an out-of-plane orientation of the magnetization.

1. Introduction

Over the past ten years the magnetic properties of multilayer systems incorporating magnetic layers have been intensively studied. The dependence of the properties on the material, crystal structure, and thickness of the layers has been investigated in an attempt to understand mechanisms and produce composite materials with desirable properties. Details of the extensive work on a variety of multilayer systems are reported in several reviews [1–3].

A property of particular interest in multilayer systems is the magnetic anisotropy energy—the energy difference between ferromagnetic moment alignment in the layer plane and out-of-plane. This interest in the anisotropy arises from the possible use of magnetic multilayers

as magneto-optical recording media, where magnetic moment alignment normal to the layers is favoured. The situation where the moments are orientated perpendicular to the plane is commonly known as perpendicular magnetic anisotropy (PMA). The geometry of a magnetic layer, however, leads to a shape-dependent demagnetizing energy, which acts to hold the moments in-plane. For an out-of-plane moment alignment to be achieved, anisotropy terms of sufficient magnitude and favouring normal spin orientation must occur. In very thin magnetic layers the so-called interface anisotropy can provide such terms. Magnetic anisotropy in multilayers has been treated in several reviews [4–6].

Multilayers composed of alternately stacked transition and rare-earth metals exhibit a large variety of novel magnetic properties, such as PMA in the Tb/Fe [7] system. The special features of these systems arise from the interesting and diverse properties of the rare-earth metals: for example the strong magnetocrystalline anisotropy, a variety of magnetic phases, and the interplay of 4f electronic states with the transition-metal 3d states.

In this work we present results for multilayers composed of cerium and iron, and cerium and an iron/cobalt/vanadium alloy. Ce is known to have 4f states that are borderline between showing localized and itinerant behaviour, which means that the electronic states depend sensitively on the local environment. It has been suggested that in Ce/transition-metal multilayers, hybridization of 4f/3d and 5d/3d electron wavefunctions will cause preferred orientation of the moments [8]. Thus it is interesting to combine Ce with Fe and FeCoV in a layered structure, to study the influence of the structure on the magnetic properties.

2. Experimental details

The multilayers were fabricated by DC magnetron sputtering in a Leybold Z600 system at PSI. The system had a base pressure of 10^{-7} mbar and the sputtering was conducted at a pressure of 1.6×10^{-3} mbar of argon. Ce/FeCoV multilayers were deposited directly onto silicon wafers, which were covered by a native amorphous SiO_2 layer. Ce/Fe multilayers were deposited onto Si wafers and also onto an iron-free polyimide substrate, Kapton. The substrates were kept at a temperature of 330 K during deposition of the layers. The sputtering rate was in the range 5–20 Å s^{-1}, and the target-to-substrate distance was 8 cm. The FeCoV alloy is of composition $Fe_{50}Co_{48}V_2$, as was verified by x-ray photoelectron spectroscopy. The Ce, Fe, and FeCoV thicknesses were in the range 10–40 Å.

Characterization of the samples was carried out using x-ray reflectivity (XRR) and high-angle x-ray diffraction (XRD). XRR measures the periodicity and interface quality of the multilayers, while XRD determines the crystal structure within the layers. The XRR and XRD were carried out at the Stanford Synchrotron Radiation Laboratory (SSRL). The measurements were performed using a focused monochromatic x-ray beam of energy 10 keV. The sample was mounted at the centre of a Huber four-circle diffractometer, and a germanium solid-state detector observed the diffracted rays. Further XRR was carried out at station 2.3 of the Synchrotron Radiation Source (SRS) at Daresbury Laboratory.

Polarized neutron reflectivity (PNR) was performed at the Rutherford-Appleton Laboratory using the CRISP reflectometer, on the ISIS pulsed neutron source. Incident neutrons have a wavelength range of 0.5–6.5 Å, and the instrument uses a time-of-flight method for determining the wavelength. The technique is sensitive to both the structural density profile and the magnetic density profile normal to the plane of the sample layers. Two reflectivity curves were measured with the incident neutron beam being polarized parallel (spin up) and antiparallel (spin down) to the sample surface. No polarization analysis was performed for the results presented here. A detailed account of the PNR technique is given in [9, 10].

For samples on silicon substrates (opaque to the ^{57}Fe 14.4 keV γ-rays), conversion-electron Mössbauer spectroscopy (CEMS) was performed at room temperature using a He/CH_4 gas flow proportional counter. The Kapton-backed multilayers, which are transparent to the γ-rays, were probed using the conventional transmission Mössbauer technique. This mode allows spectra to be obtained with the multilayers exposed to magnetic fields and maintained at temperatures as low as 4.2 K. Both methods use a conventional constant-acceleration spectrometer and a double-ramp vibration waveform so that the folded spectra appear on a flat background. Sources of ^{57}Co in Rh of up to 100 mCi were used. The spectrometer was calibrated using a 25 μm foil of α-iron at room temperature, and centre shift values are quoted relative to this standard. External fields were applied at 4.2 K by a superconducting magnet in which the field was applied normal to the plane of the multilayer and the γ-ray beam was parallel to the field direction.

3. Characterization

The crystal structure within the layers is revealed by XRD at high scattering angles. Typical XRD spectra for three Ce/Fe multilayers are shown in figure 1, in the form of θ–2θ scans. The peaks indicate that the iron layers have the bcc α-Fe structure, and are textured with the (110) planes parallel to the interfaces. The Ce layers are found to consist of fcc γ-CeHO type phase, which is textured with the (111) planes parallel to the interfaces. The CeHO phase indicates that the Ce has reacted with impurities present in the sputtering chamber. The crystalline peaks are seen down to individual layer thicknesses of 12 Å and 10 Å for the Ce and Fe layers respectively. This contrasts with previously reported results on Ce/Fe multilayers grown in UHV [11], where the Ce and Fe layers were found to be amorphous below critical thicknesses of 70 Å and 25 Å respectively. The oxygen and hydrogen impurities present in the Ce layers in our samples, and the higher base and sputtering pressures during deposition, seem to play a beneficial role in the crystallization of the Ce and Fe. Work on $CeH_{\sim 2}$/Fe multilayers [12] is in much better agreement with our results, revealing crystalline layers down to 10 Å for both

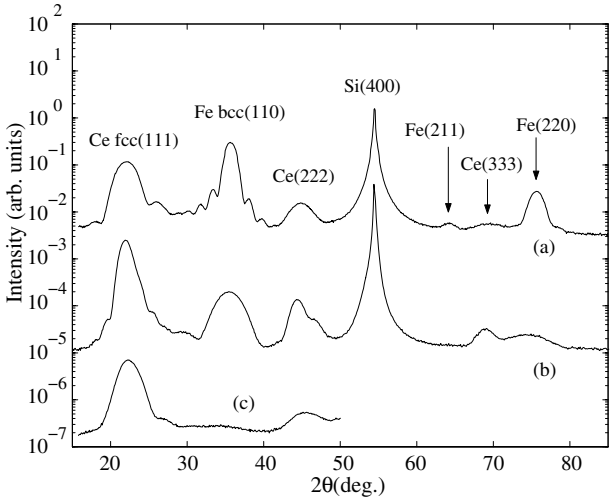

Figure 1. θ–2θ scans for Ce/Fe multilayers. (a) [Ce(20 (Å))Fe(40 (Å))]$_{40}$, (b) [Ce(40 (Å)) Fe(20 (Å))]$_{60}$, and (c) [Ce(20 (Å))Fe(10 (Å))]$_{60}$. The atomic planes producing each diffracted peak are indicated in the diagram.

$CeH_{\sim 2}$ and Fe. It has been suggested [13] that in multilayers, growth in the amorphous phase originates from a large mismatch between the interatomic distances of the adjacent metals at the interface.

For samples with decreasing layer thicknesses, the measured average lattice spacing is seen to decrease for Ce and increase for Fe. This implies that the lattice parameter at the interface differs from that for the rest of the layer, with that for Ce being smaller and that for Fe being larger. It appears that, at the interface, the Ce lattice contracts and the Fe lattice expands, in order to accommodate their mismatch.

The Ce/FeCoV multilayers show similar XRD results to the Ce/Fe multilayers. Figure 2 shows XRD spectra for two Ce/FeCoV multilayers. Indexing the peaks again leads to a fcc γ-CeHO phase and a bcc FeCoV structure with lattice spacing of 2.85 Å in agreement with that for bulk $Fe_{50}Co_{50}$ [14]. The layers are again textured with the close-packed planes parallel to the interfaces. Bragg reflections are observed down to Ce and FeCoV layer thicknesses of 10 Å and 15 Å respectively, which were the smallest thicknesses studied by XRD. Again a contraction and expansion of the lattice at the interfaces is seen in the Ce and Fe layers respectively.

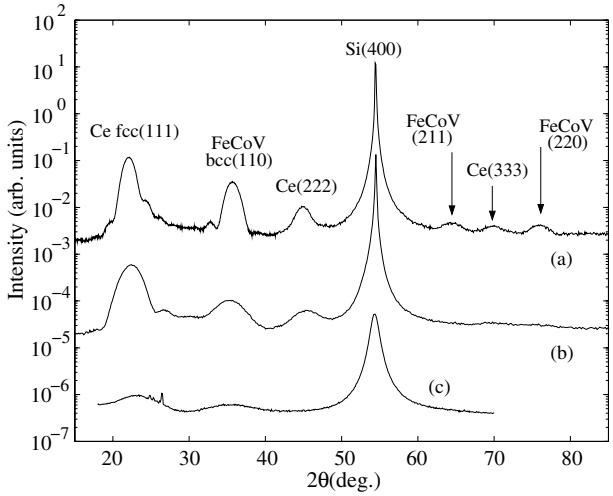

Figure 2. θ–2θ scans for Ce/FeCoV multilayers. (a) [Ce(40 (Å))FeCoV(40 (Å))]$_{40}$, (b) [Ce(20 (Å)) FeCoV(20 (Å))]$_{60}$, and (c) [Ce(10 (Å))FeCoV(15 (Å))]$_{64}$. The atomic planes producing each diffracted peak are indicated in the diagram.

The Bragg peak widths are a measure of the crystallite size in the direction normal to the interfaces. Using the Scherrer equation [15] the coherence lengths for all multilayers were calculated, and were found to be approximately equal to the individual layer thicknesses.

The multilayer periodicity and interface quality were determined by XRR. Figure 3 shows XRR curves of a Ce/Fe and a Ce/FeCoV multilayer. The curve corresponding to the Ce/FeCoV multilayer has a slow decrease of the reflected intensity as a function of the scattering angle (2θ) and sharp peaks up to the eighth order. This indicates a well-defined periodicity of the layers, and sharp interfaces in comparison to the Ce/Fe multilayer. Modelling of reflectivity profiles revealed periodicities consistent with the nominal structures. The density of the Fe and FeCoV layers was modelled and found to be consistent with bulk values, while for the Ce layers it was found to be 80% of the bulk value. This reduced Ce density is in agreement with the presence of a CeHO phase, as seen from the XRD results. The interface roughness was found to be in the range 2–5 Å for all multilayers studied.

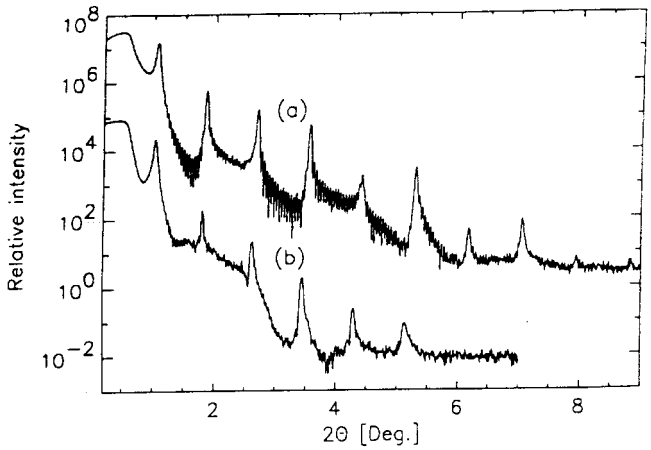

Figure 3. X-ray reflectivity curves measured at 9.5 keV for (a) [Ce(40 (Å))FeCoV(40 (Å))]$_{20}$ and (b) [Ce(40 (Å))Fe(40 (Å))]$_{20}$ multilayers.

4. Magnetic results

4.1. Polarized neutron reflectivity

Polarized neutron reflectivity (PNR) measurements provide information on the multilayer periodicity, interface roughness, and the magnetic moment magnitude. The technique is sensitive only to moments oriented in the plane of the layers. Two reflectivity curves were measured with incident neutrons being polarized parallel (spin up) or antiparallel (spin down) to the sample surface. The curves were fitted using an optical formulation code. Varying the parameters for the layer thickness and the average Fe and FeCoV magnetic moments achieved satisfactory fits to the main features of the reflectivity curves. No Ce moment was detected. It should be noted, however, that this technique is not as sensitive to the Ce layers as it is to the Fe and FeCoV, due to its smaller density. Therefore the CeHO may in fact possess a small moment.

The neutron reflectivity for a [Ce(20 (Å))FeCoV(10 (Å))]$_{60}$ multilayer is shown in figure 4, with and without an applied field in the plane of the layers. The applied-field data have been displaced for clarity. The data extend out to the first Bragg reflection. With a magnetic field of 2.3 kG applied in the plane of the layers the moments are saturated. In this situation the Bragg peak of the spin-up neutrons is more intense than that of the spin-down neutrons. This difference in reflected intensity is attributed to the in-plane magnetic moments in the FeCoV layers. For the spin-up neutrons, the total scattering length is given by the nuclear plus magnetic scattering length. For the spin-down neutrons the total scattering length is equal to the nuclear minus the magnetic scattering length, since the magnetic moments in the FeCoV layers are antiparallel to the incident neutron spin. Hence the Bragg peak is weaker in intensity for the spin-down neutrons. For the case where no field is present the Bragg peak intensities of the spin-down and spin-up neutrons are seen to be identical. This indicates the absence of any in-plane magnetization, and so implies the presence of a perpendicular magnetic anisotropy.

Modelling of the PNR data revealed periodicities close to the nominal values, interface roughness of 2–5 Å, and average moment magnitudes reduced from bulk values by an amount dependent on the magnetic layer thickness. It was seen that the thinner the layer, the smaller the average moment. This is attributed to Fe and FeCoV atoms at the interfaces having a

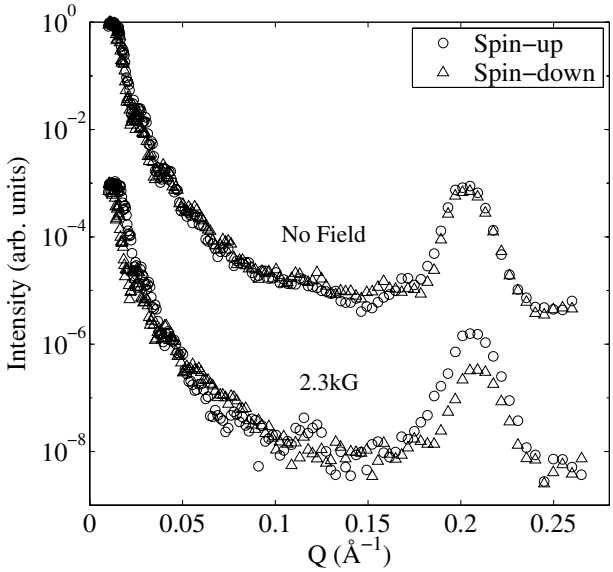

Figure 4. [Ce(20 (Å))FeCoV(10 (Å))]$_{60}$ neutron reflectivity curves without and with an applied field of 2.3 kG in the plane of the layers. For the case where no field is present the Bragg peak intensities of the spin-up and spin-down neutrons are identical, indicating the presence of a perpendicular magnetic anisotropy.

reduced moment. For thinner layers a larger proportion of atoms are at the interface, giving a smaller average moment.

4.2. Ce/Fe Mössbauer results

CEMS spectra were obtained at room temperature for the Si-backed Ce/Fe samples. The Kapton-backed Ce/Fe multilayers were studied by conventional transmission Mössbauer spectroscopy at room temperature and 4.2 K. Spectra at room temperature for [Ce(20 (Å))Fe(40 (Å))]$_{50}$ and [Ce(20 (Å))Fe(17 (Å))]$_{60}$ Si-backed multilayers are shown in figure 5, together with a reference spectrum of bulk Fe. The [Ce(20 (Å))Fe(40 (Å))]$_{50}$ spectrum is magnetically split indicating the magnetic nature of the sample. In contrast, the [Ce(20 (Å))Fe(17 (Å))]$_{60}$ spectrum consists of a magnetic sextet plus a quadrupole doublet originating from paramagnetic Fe atoms. This coexistence of magnetic and paramagnetic phases was seen in all samples with a Fe layer thickness of less than 20 Å. The transition between the two regimes seen in figure 5 occurs in a very narrow thickness range centred at 20 Å. The ratio of the areas of the magnetic and paramagnetic phases does not change with layer thickness (below the critical Fe thickness of 20 Å), being approximately in the ratio 1:1. For the Ce/Fe multilayers on Kapton substrates this coexistence is also seen below a Fe thickness of 20 Å. However, the ratio of the areas of the magnetic and paramagnetic phases does change with Fe thickness. At an Fe layer thickness of 20 Å the paramagnetic region has a very small intensity. This intensity increases as the Fe thickness decreases, until at an Fe thickness of 10 Å the spectrum consists of the paramagnetic phase alone.

All spectra were fitted with two or three components to obtain a good representation of the data. Each component represents a distinct ^{57}Fe site within the Fe layer, i.e. each with a distinct local environment. The fitted hyperfine parameters for each component for the spectra

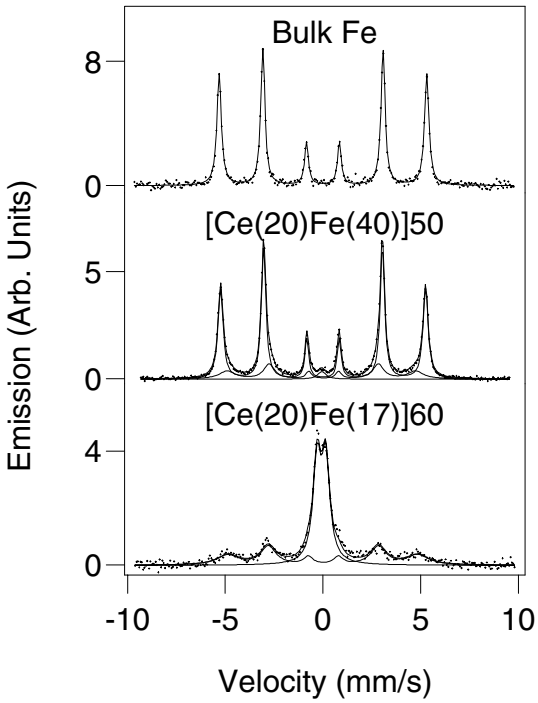

Figure 5. CEMS spectra for two Ce/Fe multilayers, obtained at room temperature. Shown for comparison is the spectrum of a 25 μm thick Fe foil.

Table 1. Fitted spectral parameters from CEMS spectra in figure 5. Errors are in brackets and are relative to last decimal place.

	Centre shift (mm s^{-1})	Quadrupole splitting (mm s^{-1})	Hyperfine field (kG)	Relative area
Bulk Fe	0	0	330	—
$[Ce(20\ (Å))Fe(40\ (Å))]_{50}$	0.00(2)	0.00(2)	325(1)	0.77(5)
	−0.02(4)	−0.12(4)	299(5)	0.21(5)
	−0.05(4)	0.0(1)	0(2)	0.02(1)
$[Ce(20\ (Å))Fe(17\ (Å))]_{60}$	0.01(4)	−0.03(4)	301(4)	0.42(3)
	−0.08(2)	0.44(2)	0(2)	0.58(3)

in figure 5 are given in table 1. The wholly ferromagnetic samples are fitted satisfactorily with two magnetic sextet components. A small paramagnetic component is required to fit the emission intensity at ∼0 mm s^{-1}, but contributes only 2% of the total area. The more intense of the sextets has a centre shift consistent with that of bcc iron at 290 K [16], but the hyperfine field is smaller by 5 kG. This component is assumed to arise from Fe atoms at the centre of the Fe layers, where all nearest neighbours are Fe atoms. The less intense sextet has broad lines and a mean hyperfine field depleted by ∼10% from that above. This component gives rise to the shoulders of the outer lines. The broad linewidth indicates a distribution of hyperfine fields. This component is thought to originate from Fe atoms at the interface with Ce.

All spectra with a coexistence of magnetic and paramagnetic phases were fitted with a broad magnetic sextet and a quadrupole-split doublet. The sextet has a hyperfine field reduced from that for bcc Fe by ∼10%. This component is thought to originate from Fe atoms at the

centre of the Fe layers. The average hyperfine field of the sextet was seen to decrease as the Fe layer thickness was reduced. The doublet has a centre shift that is small and negative, and a quadrupole splitting of 0.40 mm s^{-1} to 0.47 mm s^{-1} for the series of multilayers studied.

Measurements at 4.2 K on the Kapton-backed samples produce spectra that are magnetically ordered. No paramagnetic fraction is observed at 4.2 K. All spectra were fitted satisfactorily with one broad magnetic sextet having hyperfine parameters consistent with those for metallic iron [17]. The agreement of the hyperfine field with that for α-Fe at 4.2 K, but not at room temperature indicates that the multilayers have a reduced magnetic ordering temperature (Curie temperature, T_C). For a constant Ce thickness, T_C is seen to decrease as the Fe layer thickness decreases. The decrease in T_C can be attributed to a dilution of the Fe atoms, and a weakening of the ordering along the direction of the sample normal. In other magnetic multilayer systems a 2D-to-3D crossover in the magnetism of multilayers has been observed [18].

The 4.2 K results point to amorphous iron being at the origin of the paramagnetic doublet at room temperature. The XRD results do show Fe diffraction peaks for layer thicknesses of less than 20 Å, but these are attributed to the central crystalline region of the layers which produce the magnetically split component in the CEMS spectra. Previous Mössbauer work on Ce/Fe multilayers at room temperature, by Thiele *et al* [19], revealed a paramagnetic doublet below a critical Fe thickness of 25 Å, with similar hyperfine parameters to ours. Thiele *et al* attribute the doublet to the growth of amorphous Fe in the Fe layers.

In our results the amorphous Fe is paramagnetic at room temperature but magnetically ordered at 4.2 K in agreement with several studies on amorphous Fe [20–22]. These studies of amorphous iron (a-Fe) rely on extrapolations of experimental data obtained for a-Fe alloys containing a non-negligible amount of a second element. Xiao *et al* [20] studied two alloy types; Fe–early-transition-metal (Fe–T) and Fe–metalloid (Fe–M) systems. At room temperature some systems are seen to produce a doublet and the extrapolated parameters of a-Fe are similar to those seen in our spectra. At 4.2 K the hyperfine field of the Fe–M systems is seen to approach that of bcc α-Fe as the Fe concentration nears 100%, agreeing with that seen in our system. In the studies by Komatsu *et al* [21] and Heiman *et al* [22] Fe–rare-earth alloys were studied, including Ce. At room temperature the alloy studies predicted parameters for a-Fe which agreed very well with our measured values. At 4.2 K the magnetic moment of a-Fe was estimated to be almost the same as that of pure bcc α-Fe, and the magnetic ordering temperature was estimated at 270 K, both results agreeing with our observations.

Our 4.2 K spectra rule out the possibility of the doublet arising from alloy formation between Fe and Ce at the interfaces. The $CeFe_2$ and Ce_2Fe_{17} alloys, that are allowed by the Ce–Fe phase diagram, are paramagnetic at room temperature [23], but at 4.2 K are reported to have hyperfine fields of 169 kG and 255 kG respectively [24, 25], which are much lower than our observed field of 340 kG.

The growth of a-Fe has been seen in other Fe/rare-earth multilayers, such as Dy/Fe [26], Nd/Fe [27], and Gd/Fe [28]. Below a critical Fe thickness a collapse of the hyperfine field at room temperature is observed, which is attributed to an amorphous Fe structure in the Fe layers. The critical thickness in the Dy/Fe and Nd/Fe systems was 20 Å, and 23 Å for Gd/Fe. The hyperfine parameters of the paramagnetic components in these systems showed good agreement with those in our system at both room temperature and 4.2 K. Growth of a-Fe at the interfaces can be attributed to the mismatch between the Ce and Fe lattice structures.

Information concerning the orientation of the ordered magnetic moments in the Fe layers is contained in the relative intensities of the Mössbauer lines. Figure 6 shows CEMS spectra for three multilayers with a constant Ce thickness of 20 Å, and Fe thicknesses of 20 Å, 15 Å, and 10 Å. The intensities of the six lines are in the ratio $3{:}X{:}1{:}1{:}X{:}3$, where

$X = 4\sin^2\theta/(1+\cos^2\theta)$, and θ is the angle between the magnetic moments of the iron atoms and the incident γ-ray beam. For an Fe layer thickness of 20 Å the magnetic sextet has the ratio $X = 4$, indicating an in-plane moment orientation, i.e. $\theta = 90^\circ$. For Fe = 15 Å and 10 Å, X is smaller, indicated by the decrease in the intensity of lines 2 and 5 of the magnetic sextets. For Fe thicknesses of 20 Å, 15 Å, and 10 Å, the spectra yield angles of 90°, 60°, and 39°, respectively. Therefore, for a constant Ce thickness the Fe magnetic moments are oriented more out-of-plane as the Fe thickness decreases. The implications of this trend are considered in the discussion section.

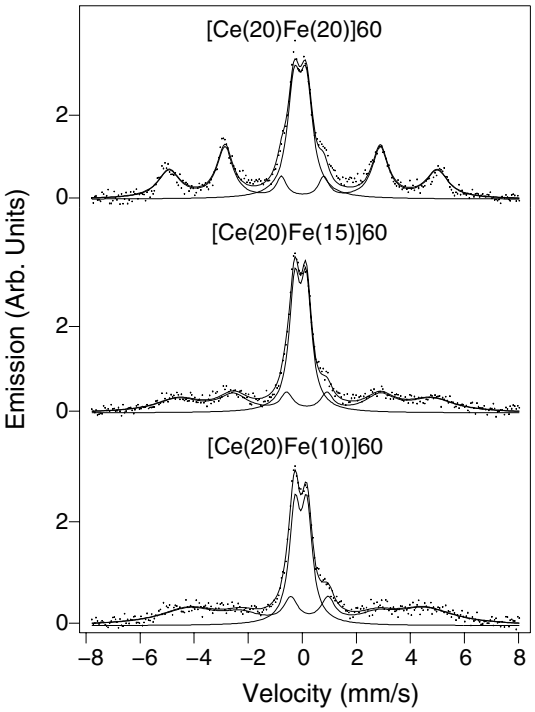

Figure 6. CEMS spectra for three Ce/Fe multilayers with a constant Ce thickness. The intensities of lines 2 and 5 of the magnetic sextets decrease as the Fe layer thickness decreases. This indicates an increased out-of-plane moment orientation as the Fe thickness decreases.

4.3. Ce/FeCoV Mössbauer results

Ce/FeCoV multilayers on silicon substrates were studied using CEMS at room temperature. Spectra for the [Ce(20 (Å))FeCoV(20 (Å))]$_{20}$, [Ce(10 (Å))FeCoV(15 (Å))]$_{64}$, and [Ce(10 (Å)) FeCoV(10 (Å))]$_{60}$ multilayers are shown in figure 7. In contrast to the Ce/Fe system, the Ce/$Fe_{50}Co_{48}V_2$ system is totally ferromagnetic at room temperature, with all spectra consisting of magnetically split sextets. The spectra were fitted with two components, one corresponding to Fe atoms at the centre of the FeCoV layers, and one originating from Fe atoms at the interface with the adjacent Ce layers. The fitted parameters for the spectra in figure 7 are presented in table 2. The component arising from atoms at the centre of the FeCoV layers has parameters that are consistent with a disordered bcc $Fe_{50}Co_{50}$ alloy [29, 30]. The sextet representing interface atoms has broad lines and a hyperfine field that is reduced from the above by ∼10%. The relative area of the sextets is found to vary with the thickness of the FeCoV layers. The area of the interface component increases as the FeCoV layer thickness decreases, as seen in other multilayer systems [31], until at a thickness of 10 Å it represents 100% of the spectrum. This trend is seen in figure 7.

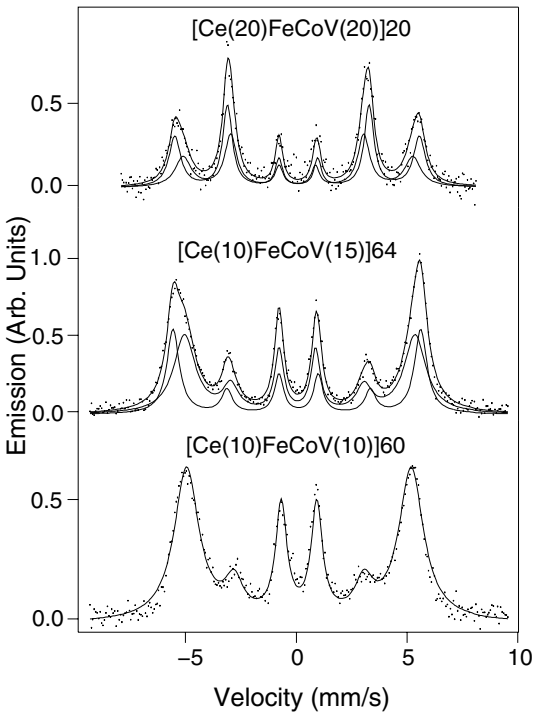

Figure 7. CEMS spectra for three Ce/FeCoV multilayers showing the transition from an in-plane to an out-of-plane moment orientation.

Table 2. Fitted spectral parameters from Ce/FeCoV CEMS spectra in figure 6. Errors are in brackets and are relative to last decimal place.

	Centre shift (mm s^{-1})	Quadrupole splitting (mm s^{-1})	Hyperfine field (kG)	Relative area
[Ce(20 (Å))FeCoV(20 (Å))]$_{20}$	0.06(4)	−0.1(1)	342(4)	0.56(10)
	0.1(1)	0.0(1)	321(7)	0.44(10)
[Ce(10 (Å))FeCoV(15 (Å))]$_{64}$	0.06(3)	−0.08(6)	346(2)	0.38(10)
	0.10(3)	0.11(6)	322(3)	0.62(10)
[Ce(10 (Å))FeCoV(10 (Å))]$_{60}$	0.12(3)	−0.01(6)	314(3)	1.0

From the spectra in figure 7, it is seen that the relative intensities of lines 2 and 5 get progressively smaller as the FeCoV thickness is reduced. For FeCoV thicknesses of 20 Å, 15 Å, and 10 Å the spectra yield angles for the magnetic moment orientation of 83°, 34°, and 28° with respect to the sample normal. The moments occupy more out-of-plane orientations as the magnetic layer thickness decreases, as was seen in the Ce/Fe system. The implications of this trend are considered in the discussion section.

4.4. Applied-field Mössbauer results—Ce/Fe multilayers

Applied-field Mössbauer spectroscopy was carried out on three multilayer samples of Ce/Fe on Kapton, [Ce(20 (Å))Fe(40 (Å))]$_{50}$, [Ce(20 (Å))Fe(20 (Å))]$_{50}$, and [Ce(30 (Å))Fe(17 (Å))]$_{50}$. In order to measure the anisotropy energy associated with rotating the magnetization of the layers out-of-plane, external fields were applied normal to the layer plane. Then the

equilibrium orientation of the iron moments was obtained from the relative intensities of the Mössbauer spectral lines. Hence, a series of magnetic field and angle values were obtained, which were used to determine the anisotropy of the multilayer. The series of spectra for the [Ce(20 (Å))Fe(40 (Å))]$_{50}$ multilayer are shown in figure 8. In zero applied field the intensities of the absorption lines for all three multilayers are in the ratio 3:4:1:1:4:3 indicating that the moments are oriented in the layer plane, i.e. $\theta = 90^\circ$. Under increasing applied fields, lines 2 and 5 become progressively weaker until the ratio is 3:0:1:1:0:3, i.e. $\theta = 0^\circ$.

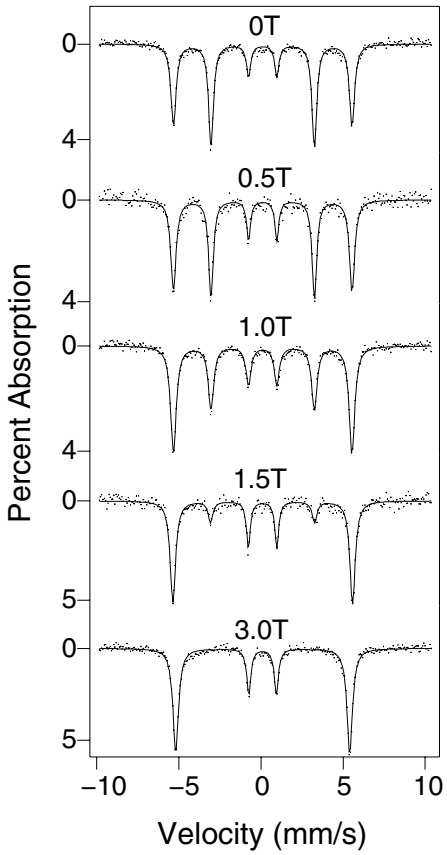

Figure 8. Mössbauer spectra for the [Ce(20 (Å))Fe(40 (Å))]$_{50}$ multilayer in a range of magnetic fields applied along the sample normal.

The dependence of the magnetic energy E of the system in an applied field B can be written as

$$E = (K_1 \sin^2\theta + K_2 \sin^4\theta) - MB\cos\theta + \frac{1}{2}\mu_0 M^2 \cos^2\theta$$

where the term in brackets represents the intrinsic anisotropy energy of the multilayer—composed of crystalline volume and interface anisotropy. The next term is the external-field energy, and the last term is the magnetostatic demagnetizing energy. K_1 and K_2 are uniaxial anisotropy constants, with the total effective anisotropy being defined as $K_{eff} = K_1 + K_2$. Positive values of K_{eff} favour an out-of-plane orientation of the magnetic moments, while negative values favour in-plane alignment. The dependence gives rise to the expression

$$B = \mu_0 M\cos\theta + \frac{4K_2}{M}\cos^3\theta - \frac{2K_1}{M}\cos\theta - \frac{4K_2}{M}\cos\theta$$

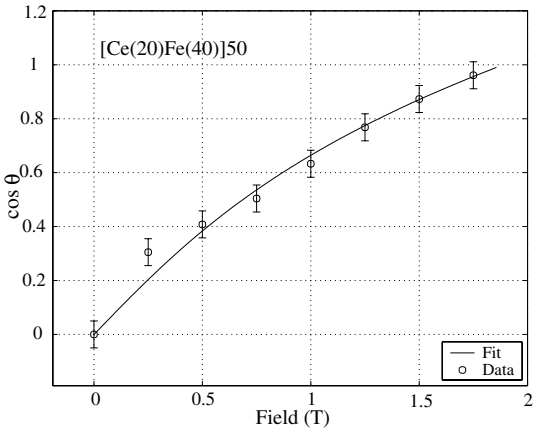

Figure 9. Values of $\cos\theta$ against applied field for the [Ce(20 (Å))Fe(40 (Å))]$_{50}$ multilayer. The $\cos\theta$ values are calculated from each spectrum in figure 8. A fit to the data is shown which yields values of K_1 and K_2.

relating the equilibrium orientation of the moment, θ, to the applied field B. The B against $\cos\theta$ data for each sample were fitted using the above equation to yield values of K_1 and K_2. The experimental points taken from the spectra of figure 8 are shown in figure 9, with such a fit. K_{eff}-values calculated from the fits are presented in table 3.

Table 3. Calculated intrinsic anisotropy values.

Multilayer	K_{eff} (10^5 J m^{-3})
[Ce(20 (Å))Fe(40 (Å))]$_{50}$	5.9 ± 0.5
[Ce(20 (Å))Fe(20 (Å))]$_{50}$	11.1 ± 1.0
[Ce(30 (Å))Fe(17 (Å))]$_{50}$	12.0 ± 1.5

The positive sign for K_{eff}, seen for all three multilayers, indicates a preference for an out-of-plane orientation of the moments. This intrinsic anisotropy K_{eff} adds to the demagnetizing energy to give the total anisotropy energy. The demagnetizing energy $(-(1/2)\mu_0 M^2)$ is -1.96×10^6 J m^{-3}, assuming the saturated α-Fe value for M, and so the total anisotropy energy for these three multilayers is negative, and favours in-plane moment alignment. Therefore in zero applied field, we expect an in-plane moment orientation, as observed in these samples. Analysis of the intrinsic anisotropy energies into volume and interface contributions is treated in the discussion section.

5. Discussion

5.1. Ce/Fe and Ce/FeCoV CEMS measurements

The total magnetic anisotropy energy of a magnetic layer is conventionally split into a component dependent on bulk anisotropies K_V, and on anisotropy arising from interface interactions K_S, which obey the relation [32]

$$K = K_V + \frac{2K_S}{t} - \frac{1}{2}\mu_0 M^2$$

where t is the magnetic layer thickness, and $-(1/2)\mu_0 M^2$ is the demagnetizing energy that in this analysis appears explicitly from K_V (in other studies it is included in the volume contribution to the anisotropy). In the equation the factor 2 arises since the layer is bounded by two interfaces. In the convention used here, a positive K indicates a preferred direction of the

magnetization that is perpendicular to the layer plane. For a magnetic layer the demagnetizing energy is nearly always the dominant energy, and so K is negative and in-plane moments are observed. However, if the layer thickness t is small enough, the relative contribution to K from interface effects can outweigh the demagnetizing term. In this case, if K_S is positive (favouring out-of-plane moments), K will be positive and a PMA will result.

In both the Ce/Fe and Ce/FeCoV systems we observe a transition from in-plane alignment to out-of-plane alignment of the moments as the magnetic layer thickness is reduced. The observation of this trend indicates that the Ce/Fe and Ce/FeCoV interface interactions favour an out-of-plane moment orientation, i.e. K_S is positive. The magnitude of K_S can be calculated using the effective anisotropy energy, which is found from applied-field measurements.

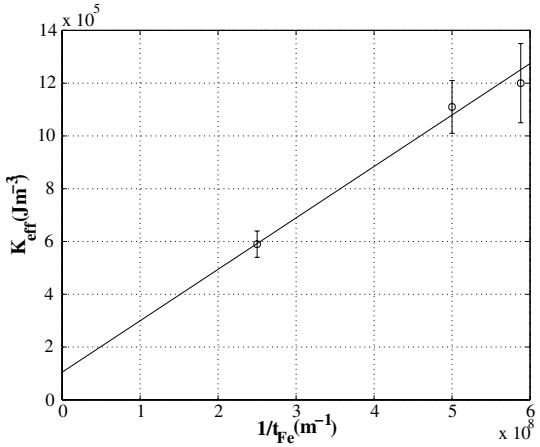

Figure 10. Variation of the effective anisotropy energy K_{eff} with $1/t$ for Ce/Fe multilayers, where t is the Fe layer thickness. The values of K_V and K_S are obtained from the intercept on the K_{eff}-axis and slope respectively.

5.2. Ce/Fe anisotropy energies

Measurements of the intrinsic anisotropy K_{eff} on a series of Ce/Fe multilayers with different magnetic layer thickness allow evaluation of K_V and K_S using the relation

$$K_{eff} = K_V + \frac{2K_S}{t}.$$

K_{eff} is the total anisotropy without the demagnetizing contribution. The demagnetizing energy was included explicitly in the expression used to fit the applied-field data, and find K_{eff}. The variation of the measured values of K_{eff} against $1/t$ is shown in figure 10. The fitted line gives values of $K_V = 1.1\ (\pm 1.2) \times 10^5$ J m^{-3} and $K_S = 0.98\ (\pm 0.15) \times 10^{-3}$ J m^{-2}. The value of K_V is consistent with the magnetocrystalline bulk anisotropy for bcc iron, 4.1×10^4 J m^{-3}. The positive value of K_S indicates that the Ce/Fe interface does indeed favour an out-of-plane alignment of the moments. Collected literature values for Fe/transition-metal multilayers [6] indicate that interfaces with Fe produce positive values for K_S in general. The magnitude of our measured K_S for Ce/Fe is comparable with the largest reported in [6], indicating a strong out-of-plane anisotropy for the Ce/Fe interface.

For Ce/FeCoV interfaces an even larger value of K_S is predicted. In zero applied field, for similar magnetic layer thicknesses the moments in the Ce/FeCoV system are observed to be more out-of-plane than those in Ce/Fe. Since the moment magnitudes for Fe and FeCoV

are similar, the demagnetizing energies of their layers are similar. Therefore, the moments of each system are constrained to be in-plane by demagnetizing energies with similar strengths. Therefore, the observation that the moments are more out-of-plane in the FeCoV layers than in the Fe layers indicates a larger interface anisotropy in the Ce/FeCoV system.

Acknowledgments

The work was funded by an EPSRC grant. G S Case and D Mannix were supported by EPSRC research studentships.

References

[1] Falicov L M *et al* 1990 *J. Mater. Res.* **5** 1299
[2] Gradmann U 1993 *Handbook of Magnetic Materials* vol 7 (Amsterdam: Elsevier) pp 1–95
[3] Bland J A C and Heinrich B (ed) 1994 *Ultrathin Magnetic Structures* vols 1, 2 (Berlin: Springer)
[4] den Broeder F J A *et al* 1991 *J. Magn. Magn. Mater.* **93** 562
[5] Johnson M T *et al* 1996 *Rep. Prog. Phys.* **59** 1409
[6] Heinrich B *et al* 1993 *Adv. Phys.* **42** 523
[7] Sato N 1986 *J. Appl. Phys.* **59** 2514
[8] Yang Y J *et al* 1991 *Phys. Rev.* B **44** 5132
[9] Felcher G P 1993 *Physica* B **192** 137
[10] Zabel H 1994 *Physica* B **198** 156
[11] Klose F *et al* 1993 *J. Appl. Phys.* **74** 1040
[12] Schulte O *et al* 1995 *Phys. Rev.* B **32** 6480
[13] Landes J *et al* 1991 *Phys. Rev.* B **44** 8342
[14] Shiga M 1972 *IEEE Trans. Magn.* **8** 666
[15] Warren B E 1969 *X-Ray Diffraction* (Reading, MA: Addison-Wesley)
[16] Violet C E *et al* 1971 *J. Appl. Phys.* **42** 4339
[17] Johnson C E *et al* 1963 *Proc. Phys. Soc.* **81** 1079
[18] Gutierrez C J *et al* 1991 *J. Magn. Magn. Mater.* **93** 326
[19] Thiele J *et al* 1993 *J. Magn. Magn. Mater.* **119** 141
[20] Xiao G *et al* 1987 *Phys. Rev.* B **35** 8763
[21] Komatsu H *et al* 1993 *Nucl. Instrum. Methods* B **76** 89
[22] Heiman N *et al* 1975 *Phys. Lett.* A **55** 297
[23] Buschow K H J *et al* 1970 *Phys. Status Solidi* **42** 231
[24] Pokatilov V S 1998 *J. Magn. Magn. Mater.* **189** 189
[25] Roulin G *et al* 1994 *Hyperfine Interact.* **88** 65
[26] Yoden K *et al* 1998 *Japan. J. Appl. Phys.* **27** 1680
[27] Mibu K *et al* 1990 *Hyperfine Interact.* **54** 831
[28] Landes J *et al* 1991 *Phys. Rev.* B **44** 8342
[29] Johnson C E *et al* 1961 *Phys. Rev. Lett.* **6** 450
[30] de Mayo B *et al* 1970 *J. Appl. Phys.* **41** 1319
[31] Bakkaloglu Ö F *et al* 1993 *J. Magn. Magn. Mater.* **125** 221
[32] Draaisma H J G *et al* 1987 *J. Magn. Magn. Mater.* **66** 351